Atmospheric Research 135–136 (2014) 48–58

Contents lists available at ScienceDirect

Atmospheric Research

journal homepage: www.elsevier.com/locate/atmos

Impact of $PM_{2.5}$ chemical compositions on aerosol light scattering in Guangzhou — the largest megacity in South China

Jun Tao [a,b], Leiming Zhang [b,c], Kinfai Ho [d,*], Renjian Zhang [b,*], Zejian Lin [a], Zhisheng Zhang [a], Mang Lin [a], Junji Cao [e], Suixing Liu [e], Gehui Wang [e]

[a] South China Institute of Environmental Sciences, Ministry of Environmental Protection, Guangzhou, China
[b] RCE-TEA, Institute of Atmospheric Physics, Chinese Academy of Sciences, Beijing, China
[c] Air Quality Research Division, Science Technology Branch, Environment Canada, Toronto, Canada
[d] School of Public Health and Primary Care, The Chinese University of Hong Kong, Hong Kong, China
[e] Key Laboratory of Aerosol, SKLLQG, Institute of Earth Environment, Chinese Academy of Sciences, Xi'an, China

ARTICLE INFO

Article history:
Received 1 February 2013
Received in revised form 28 August 2013
Accepted 28 August 2013

Keywords:
$PM_{2.5}$
Aerosol chemical composition
Aerosol scattering coefficient
Urban aerosols

ABSTRACT

Daily $PM_{2.5}$ samples were collected in Guangzhou — the largest megacity in South China, for a period of one month in each season during 2009–2010. Mass concentrations of water-soluble inorganic ions, organic carbon (OC) and elemental carbon (EC) in $PM_{2.5}$ were determined, and aerosol scattering coefficient (b_{sp}) was synchronously measured. The daily $PM_{2.5}$ mass concentrations ranged from 21.0 to 213.6 μg m^{-3} with an annual average of 76.8 ± 41.5 μg m^{-3}. The highest seasonal average $PM_{2.5}$ was observed in winter (103.3 ± 50.1 μg m^{-3}) and the lowest in summer (38.6 ± 15.7 μg m^{-3}). Annual average $PM_{2.5}$ mass scattering efficiency (MSE) was 3.5 ± 0.9 m^2 g^{-1}, with obvious seasonal variations in sequence of autumn (4.5 ± 0.2 m^2 g^{-1}) > winter (3.9 ± 0.5 m^2 g^{-1}) > spring (3.0 ± 0.4 m^2 g^{-1}) > summer (2.3 ± 0.3 m^2 g^{-1}).

To determine the relationship between b_{sp} and the chemical components of $PM_{2.5}$, b_{sp} was reconstructed in each season using the original IMPROVE formula with a modification of including sea salt aerosols. The estimated b_{sp} using this method was 22 ± 28% smaller on annual average compared to the measurements. Multiple linear regression of measured b_{sp} against $(NH_4)_2SO_4$, NH_4NO_3, OM (Organic Mass), SS (Sea Salt), FS (Fine Soil), and CM (Coarse Mass) were also performed in all the four seasons. The estimated b_{sp} from using the regression equation was 4 ± 12% larger than the measured values. On average, $(NH_4)_2SO_4$, NH_4NO_3, OM, SS, FS and CM accounted for 50 ± 11%, 18 ± 10%, 19 ± 5%, 5 ± 4%, 3 ± 2% and 5 ± 6%, respectively, of the estimated b_{sp}.

1. Introduction

Fine particulate matter with aerodynamic diameter (D_a) smaller than 2.5 μm ($PM_{2.5}$) has been found to adversely impact human health (Dockery and Pope, 1994; Laden et al., 2000; Samet et al., 2000; Pope and Dockery, 2006) and visibility (Malm et al., 1994; Watson, 2002; Lowenthal and Kumar, 2004). With the increase of public awareness about visibility degradation or hazy weather, China Ministry of Environmental Protection promulgated $PM_{2.5}$ standard in early 2012. As a matter of fact, hazy weather can still occur even when daily $PM_{2.5}$ concentrations satisfy the newly established standard. Health impact due to poor air quality and visual perception are mostly concerned by general public nowadays. Therefore, identification of dominant pollutant species in ambient air is crucial for making pollution control policies to improve visibility degradation. To date, integrated and systematic monitoring network aiming at visibility investigation similar to the IMPROVE network has not yet been established in

* Corresponding authors.
E-mail addresses: kfho@cuhk.edu.hk (K. Ho), zrj@tea.ac.cn (R. Zhang).

0169-8095/$ – see front matter © 2013 Elsevier B.V. All rights reserved.
http://dx.doi.org/10.1016/j.atmosres.2013.08.015

China, although a network with 31 rural sites and 14 background monitoring sites is currently under construction. Almost all existing ambient air monitoring sites in China are situated in urban areas, in contrast to IMPROVE network which was designed for rural areas.

Haze frequently occurred in the Pearl River Delta (PRD) region of China during the recent decades, especially in megacities like Guangzhou (Andreae et al., 2008; Deng et al., 2008; Tan et al., 2009; Yao et al., 2010). Aerosol optical properties are important parameters in haze phenomena. For example, light extinction (b_{ext}) is an index directly reflecting visibility degradation, which includes light scattering by particles (b_{sp}) and gases (b_{sg}), and light absorption by particles (b_{ap}) and gases (b_{ag}). b_{ext} can be estimated using Mie theory through measuring particle size distribution in ambient air and associated particle refraction index (Watson et al., 2008). Such a method was used by Cheng et al. (2008) to estimate b_{ext} at a suburban site of Guangzhou. However, continuous long-term measurements of particle size distribution and chemical composition are difficult to achieve. An alternative could be use of the IMPROVE formula — the original and/or the revised ones, to estimate b_{ext} based on the chemical compositions of $PM_{2.5}$, PM_{10} and NO_2 (Watson, 2002). One issue of adopting this method is that both the original and the revised formula were developed for rural/remote areas where PM concentrations were low and may not be applicable to urban environments such as in Guangzhou where the PM concentrations were extremely high.

The original IMPROVE formula was found to systematically overestimate b_{ext} by 34% at the IMPROVE regional network sites due to the overestimated dry mass scattering efficiencies (MSEs) for $(NH_4)_2SO_4$ and NH_4NO_3 (Lowenthal and Kumar, 2003). The revised formula was subsequently developed based on the 21 IMPROVE remote sites to reduce biases in light extinction estimation (Pitchford et al., 2007). Both the original and the revised formulas have been applied to various urban locations in China. None of the studies adopting the original IMPROVE formula evaluated its applicability to urban environment due to the lack of online measured b_{ext} data (Cheung et al., 2005; Yang et al., 2007; Tao et al., 2009; Zhang et al., 2012). A few other studies adopting the revised formula found that the formula overestimated b_{ext} by 36.7% in Guangzhou urban area (Jung et al., 2009a),underestimated b_{ext} by almost 5.0% in Beijing (Jung et al., 2009b), and underestimated b_{ext} by almost 15.0% in Xi'an urban area (Cao et al., 2012). It seems that the revised formula might not be appropriate for applications in urban environments in China. To date, there is no study covering all different seasons reconstructing b_{sp} based on $PM_{2.5}$ chemical compositions in South China urban areas.

The present study aims to reach a few goals. The first goal is to understand PM levels and visibility related aerosol optical properties in Guangzhou through direct field measurements. The second one is to evaluate the applicability of the original IMPROVE formula to the calculation of light scattering in this urban environment. And the third goal is to assess the contributions of individual components of $PM_{2.5}$ to the total light scattering making use of a multiple linear regression model. These goals are set due to the following reasons: (1) there is a lack of information concerning the seasonal characteristics of the aerosol optical properties; (2) the original IMPROVE formula is a simpler and more practical approach than the Mie theory in calculating light scattering and is worth to be evaluated using field data collected in this study; and (3) there is no systematic study on the light scattering mechanisms of particles in China and thus a lack of knowledge of the dominating contributors to the light scattering. Results presented in this study will shed some light on each of the above goals.

2. Methodology

2.1. Site description

The monitoring station (23°07′N,113°21′E; see Fig. 1) is situated in the South China Institute of Environmental Science (SCIES) which is located in an urban district of Guangzhou, the largest megacity of South China. There is no obvious industrial activity near the monitoring station. The instruments used in this study were installed on the roof (50 m above ground) of the building in the SCIES complex. More information about this station can be found in Tao et al. (2012).

2.2. Continuous measurements of aerosol scattering coefficient, meteorological parameters, and routine air pollutants

b_{sp} was measured using an integrating nephelometer (TSI Incorporated, Shoreview, MN, U.S.A., Model 3563) in three wavelengths: 450 nm (blue), 550 nm (green), and 700 nm (red). b_{sp} data in 550 nm were used in this study. This nephelometer was equipped with a conventional total suspended particulate (TSP) cyclone. The flow rate was set at 20 L min^{-1} for drawing air through a temperature-controlled inlet. The heated inlet in the nephelometer controlled the relative humidity (RH) of inflow air to be less than 70% to reduce the influence of water vapor on b_{sp}. The data averaging time was 1 min. Calibration of the nephelometer was performed every week using carbon dioxide (CO_2) as high-span gas and filtered air as low-span gas. The baseline (zero level) data was measured for 5 min after each 60-min sample as background value. The result of total b_{sp} was corrected for Angular Nonidealities following the method described in previous studies (Anderson and Ogren, 1998; Lin et al., 2013). The nephelometer truncation error was expected to be around 5% considering that the majority of particles had a D_a smaller than 1 μm at the SCIES site (Lin et al., 2013).

Meteorological parameters, including visibility (VIS), wind direction (WD), wind speed (WS), RH, temperature (TEMP), solar radiation (SR) and precipitation (PR), were measured every 30 min. Visibility was measured using a present weather detector (Vaisala Company, Helsinki, Finland, Model PWD22). Wind direction and wind speed were recorded by the wind monitor (Vaisala Company, Helsinki, Finland, Model QMW110A). Ambient RH and TEMP were measured by an RH/TEMP probe (Vaisala Company, Helsinki, Finland, Model QMH102). Solar radiation was measured by a Pyranometer (Kipp & Zonen Inc., Delft, Netherlands, Model CMP21) and precipitation was measured by a rain gauge (Vaisala Company, Helsinki, Finland, Model RG13). Both

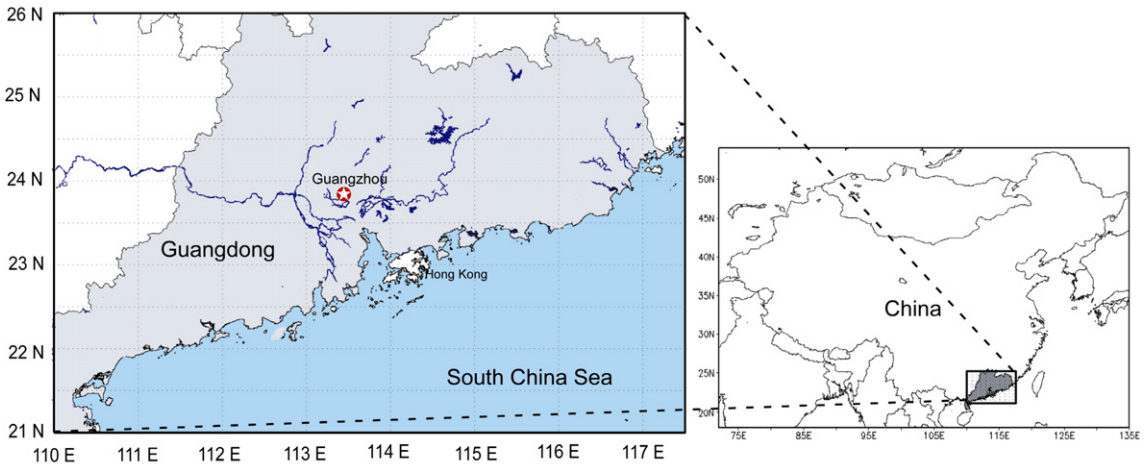

Fig. 1. The geographic location of the sampling site.

meteorological instruments were mounted 3 m above the roof of the station (53 m above ground).

Trace gases including sulfur dioxide (SO_2) and nitrogen oxides (NO_x) were measured every 5 min, by a SO_2 analyzer and NO–NO_2–NO_x analyzer (Thermo Fisher Scientific Inc., Franklin, MA; Model 43i, Model 42i), respectively. All gas analyzers were calibrated weekly (Tao et al., 2012). Due to the lack of PM_{10} concentration data at the SCIES site, daily PM_{10} concentrations were obtained from the Guangdong Shangxueyuan national environmental monitoring site, located 2.0 km south of the SCIES site.

2.3. Sample collection and artifacts

Daily 24-h integrated $PM_{2.5}$ (from 10:00 am to 9:30 am the next day, local time) samples were collected with 47 mm quartz microfiber filters (Whatman International Ltd., Maidstone, England, Q-MA) using an aerosol sampler (BGI Incorporated, Waltham, MA, U.S.A., Model PQ200). This sampler was equipped with a very sharp cut cyclone (Model VSCC) that separated the particles with aerodynamic diameter less than 2.5 μm when a vacuum pump draws air at a flow rate of 16.7 L min^{-1}. The airstream was connected to the 47 mm quartz filters (Whatman International Ltd., Maidstone, England, Q-MA). Before sampling, the quartz filters were baked at 800 °C for 3 h to remove adsorbed organic vapors and then equilibrated in desiccators for 24 h. Furthermore, the flow rate of the $PM_{2.5}$ sampler was calibrated prior to the sampling. The filter samples were stored in a freezer at −18 °C before chemical analysis to minimize the evaporation of volatile components. The quartz filters were analyzed gravimetrically for particle mass concentrations using a Sartorius MC5 electronic microbalance with a sensitivity of ±1 μg (Sartorius, Göttingen, Germany) after 24-h equilibration at a temperature between 20 °C and 23 °C and an RH between 35% and 45%. Each filter was weighed at least three times before and after sampling, and the net mass was obtained by subtracting the average of the pre-sampling weights from the average of the post-sampling weights. Differences among replicate weights were less than 20 μg for each sample. Also, field blank was collected every ten samples for 24 h without pump on. A total of 12 field blanks had been obtained in this study. The field blanks were analyzed for correcting sampling artifacts with quartz filters. Quartz filters of OC, EC and water soluble ions were corrected for positive artifacts using blank values.

In the IMPROVE network, nylon filters were typically used for ion analysis, and were preceded with a denuder designed to capture acidic gases (such as HNO_3, HNO_2, SO_2, and HCl). There, Teflon filters were used for weighing $PM_{2.5}$ mass concentrations and quartz filters were only used for carbon analysis. In the present study, $PM_{2.5C}$samples were all collected on quartz filters without adding a denuder and were then analyzed for mass, carbon, and water soluble ions. However, the inlet of the Federal Reference Method (FRM) sampler (such as PQ200 sampler) could act as an efficient denuder for HNO_3 (Chow et al., 2005), although evaporative losses of ammonium nitrate on quartz filter might slightly bias nitrate and $PM_{2.5}$ mass concentrations.

2.4. Chemical analysis

A 0.5 cm^2 punch from each quartz filter was analyzed for eight carbon fractions following the IMPROVE_A thermal/optical reflectance (TOR) protocol on a DRI model 2001 carbon analyzer (Atmoslytic Inc., Calabasas, CA, USA) (Cao et al., 2003; Chow et al., 2007). This analysis produced four OC fractions (OC1, OC2, OC3, and OC4 at 140 °C, 280 °C, 480 °C, and 580 °C, respectively, in a helium [He] atmosphere), OP (a pyrolyzed carbon fraction determined when transmitted laser light attained its original intensity after oxygen [O_2] was added to the analysis atmosphere), and three EC fractions (EC1, EC2, and EC3 at 580 °C, 740 °C, and 840 °C, respectively, in a 2% O_2/98% He atmosphere). IMPROVE_TOR OC is operationally defined as OC1 + OC2 + OC3 + OC4 + OP and EC is defined as EC1 + EC2 + EC3-OP (Chow et al., 2007). Inter-laboratory comparisons of samples between IMPROVE_TOR protocol and the TMO (thermal manganese dioxide oxidation) approach showed a difference of <5% for TC and <10% for OC and EC (Cao et al., 2003).

One-fourth of each quartz filter sample was used to determine the water-soluble ion concentrations. Four anions (SO_4^{2-}, NO_3^-, Cl^-, and F^-) and five cations (Na^+, NH_4^+, K^+,

Mg^{2+}, and Ca^{2+}) were determined in aqueous extracts of the filters by ion chromatography (IC, Dionex DX-600, Dionex Corp., Sunnyvale, CA, USA). The extraction of water-soluble species from the quartz filters was achieved by placing the cut portion (1/4) of each filter into a separate 20 mL vial, followed by 10 mL distilled–deionized water (with a resistivity of >18 MΩ), and then subjected to ultrasonic agitation for 1 h as well as additional shaking (using a mechanical shaker) for 1 h for complete extraction of the ionic compounds. The extract solutions were filtered (0.25 μm, PTFE, Whatman International Ltd., USA) and stored at 4 °C in pre-cleaned tubes until analysis. Cation (Na^+, NH_4^+, K^+, Mg^{2+}, and Ca^{2+}) concentrations were determined by using a CS12A column (Dionex Corp.) with 20 mM MSA eluent. Anions (SO_4^{2-}, NO_3^-, Cl^-, and F^-) were separated on an AS11-HC column (Dionex Corp.) with 20 mM KOH eluent. A calibration was performed for each analytical sequence. The detection limits (DL) of cations and anions were within the range of 0.0021–0.0126 μg cm^{-2} and 0.0215–0.0676 μg cm^{-2}, respectively. Standard Reference Materials (SRMs) obtained from the National Research Center for Certified Reference Materials, China, were analyzed for quality assurance purposes. Procedural blank values were subtracted from sample concentrations (Shen et al., 2009; Zhang et al., 2011).

2.5. Data analysis method

To investigate the contributions of individual $PM_{2.5}$ chemical components to b_{sp}, the original IMPROVE formula was applied in the present study (Pitchford et al., 2007). The formula can be simplified as:

$$b_{sp} = 3 \times f(RH) \times [(NH_4)_2SO_4] + 3 \times f(RH) \times [NH_4NO_3] + 4 \times [OM] + 1.0 \times [FS] + 0.6 \times [CM]. \quad (1)$$

Considering the significant impact of sea salt aerosols from the South China Sea on urban aerosols in Guangzhou, the above formula was modified to include sea salt contributions (Pitchford et al., 2007):

$$b_{sp} = 3 \times f_L(RH) \times [(NH_4)_2SO_4] + 3 \times f_L(RH) \times [NH_4NO_3] + 4 \times [OM] + 1.7 \times f_{SS} \times [SS] + 1.0 \times [FS] + 0.6 \times [CM] \quad (2)$$

where $[(NH_4)_2SO_4] = 1.375[SO_4^{2-}]$; $[NH_4NO_3] = 1.29[NO_3^-]$; $[OM] = 1.4\ [OC]$ (see the choice of conversion factor in Section 3.1); $[SS] = 1.8\ [Cl^-]$; [FS] is soil concentration ($[FS] = 2.2[Al] + 2.49[Si] + 1.63[Ca] + 2.42[Fe] + 1.94[Ti]$); $[CM] = [PM_{10}] - [PM_{2.5}]$. b_{sp} and mass concentrations are given in units of Mm^{-1} and μg m^{-3}, respectively. RH growth curves of $f_L(RH)$ and $f_{SS}(RH)$ of sulfate, nitrate, and SS can be referred to (Pitchford et al., 2007). Considering that most of the sulfate and nitrate mass distributed in droplet mode (Yu et al., 2010), we used $f_L(RH)$ rather than $f_S(RH)$ in this study. Due to the lack of soil element measurements, we assumed that Ca^{2+} is 5% of FS mass based on many previous soil source profiles (Aldabe et al., 2011; Amato and Hopke, 2012; Tao et al., 2013). Thus, $[FS] = 20\ [Ca^{2+}]$.

3. Results and discussion

3.1. $PM_{2.5}$ chemical compositions

The annual average $PM_{2.5}$ mass concentration was 76.8 ± 41.5 μg m^{-3}, which was more than two times of the China National Ambient Air Quality Standards (GB3095-2012) for annual $PM_{2.5}$ (35 μg m^{-3}). The $PM_{2.5}$ level in urban Guangzhou was slightly lower than in the other mega cities in China where measurements were available, e.g., Xiamen (86.2 μg m^{-3}) (Zhang et al., 2012), Shanghai (90.3 μg m^{-3}) (Feng et al., 2009), Beijing (96.6 μg m^{-3}) (Duan et al., 2006), Chengdu (165.1 μg m^{-3}) (Tao et al., 2013), and Xi'an (194.1 μg m^{-3}) (Zhang et al., 2011).

Daily concentrations of $PM_{2.5}$ ranged from 21.0 to 213.6 μg m^{-3} (Fig. 2). Evident seasonal variations were observed (Table 1), which showed winter (103.3 μg m^{-3}) > autumn (89.3 μg m^{-3}) > spring (76.0 μg m^{-3}) > summer (38.6 μg m^{-3}). The $PM_{2.5}$ level should be affected by emission sources, transportation, chemical transformation, and depositional processes. Meteorological conditions affect almost all of these processes. According to the air pollutant emission inventory in PRD (Zheng et al., 2009), about 91.4% of SO_2 emissions were from power plant and industrial sources, 87.2% of NO_x emissions were from power plant and mobile sources, and 97.2% of primary $PM_{2.5}$ emissions were from industrial, mobile and power plant sources in this region. Since SO_2 and NO_x are important gaseous precursors for $PM_{2.5}$, industrial sources, power plant emissions and mobile sources should be the main sources of $PM_{2.5}$ in PRD. The causes of the seasonal variations in $PM_{2.5}$ were explained below in terms of seasonal variations of emissions and metrology-driven processes.

The highest seasonal $PM_{2.5}$ was observed in winter and should be caused by a combination of low wind speed (thus slow horizontal diffusion), weak solar radiation (thus low mixing height), and relatively low precipitation (thus low wet deposition amount). Seasonal variations of emissions should not be a factor since emissions from almost all industrial sources and power plant emissions were lowest in January among all the months (Zheng et al., 2009) and monthly variations of mobile source emissions were relatively small. The second highest seasonal $PM_{2.5}$ level in autumn was due to the lowest seasonal wind speed and the relatively high industrial source emission. For example, the power plant emissions were highest in October (Zheng et al., 2009); this combined with favorable meteorological conditions (lower wind speed and precipitation) for sulfate formation explained the highest seasonal sulfate concentration (27.5 ± 8.7 μg m^{-3}, or 30.8% of $PM_{2.5}$) in autumn among all the seasons (Table 1).

The lowest seasonal $PM_{2.5}$ was observed in summer and was only one-third to one-half of those in other seasons. The lowest seasonal sulfate was also in summer. The observed phenomena are contradictory to the quite high emissions in July from most industrial sources and power plants, and to the strong solar radiation conditions which favored sulfate formation. High mixing heights in summer should have played a role in reducing surface layer sulfate and $PM_{2.5}$ concentrations. In addition, air masses affected by summer monsoon from the South China Sea introduced clean air into the city. The second lowest seasonal $PM_{2.5}$ was observed in

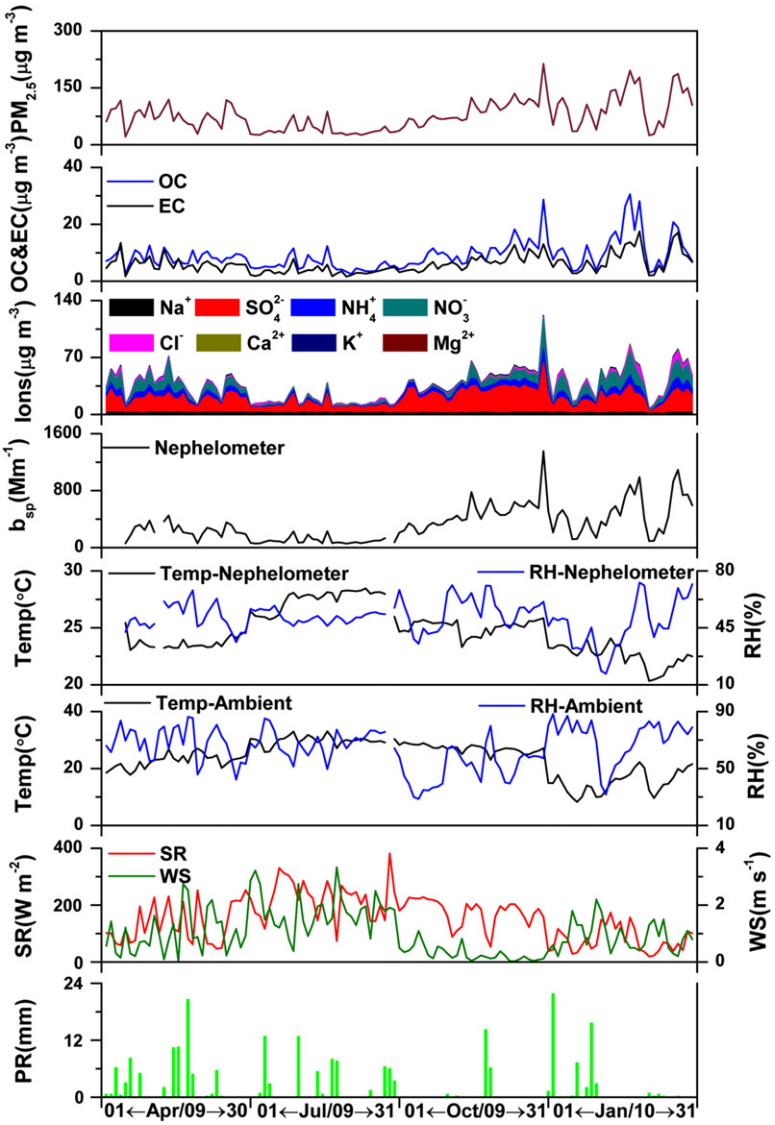

Fig. 2. Temporal variations of daily $PM_{2.5}$ mass concentrations, its chemical components, b_{sp}, and selected meteorological parameters in four seasons (2009–2010).

spring, but it doubled the summer level despite the lower emissions in April than in July (Zheng et al., 2009). Weaker solar radiation in spring did not favor sulfate formation, but also caused low mixing height. It should be pointed out that spring had more precipitation than any other seasons, yet not lower $PM_{2.5}$ level than in summer. This was likely because precipitation scavenging was not very efficient for removing fine particles from the atmosphere, although efficient for removing coarse particle (Wang et al., 2010).

OC and EC were important components of $PM_{2.5}$, accounting for 12.3 ± 3.0% and 8.1 ± 1.8%, respectively, of the annual $PM_{2.5}$ mass concentration. The seasonal variations of OC and EC were similar to those of $PM_{2.5}$ mass, following the sequence of winter > autumn > spring > summer. The sources of carbonaceous aerosols can be qualitatively evaluated with the relationship between OC and EC concentrations (Turpin and Huntzicker, 1995; Cao et al., 2007; Zhang et al., 2007). As shown in Fig. 3, the correlations between OC and EC in spring ($R^2 = 0.64$) and summer ($R^2 = 0.58$) were not as good as in autumn and winter ($R^2 = 0.75$ and 0.83, respectively). Thus, significant fractions of OC and EC, and more fractions in autumn and winter than in spring and summer, were likely derived from the same sources. On the other hand, significant differences in OC/EC ratios between coal combustion (2.7), vehicle emissions (1.1), and biomass burning (9.0) were found by Watson et al. (2001). As expected, the OC/EC ratios in this study were lower than 2.0 in all seasons. This indicates that vehicle emission played an important role in particulate carbonaceous pollution in Guangzhou.

Vehicle emissions have been identified as the major source of NO_x in the urban area of PRD (Zheng et al., 2009). Thus, NO_x could be roughly regarded as the tracer of vehicle emissions. Good correlations between OC and NO_2 were also found in autumn and winter ($R^2 = 0.73$ and 0.80, respectively), but not so good in spring and summer ($R^2 = 0.45$ and 0.64, respectively) (figure not shown). However, a strong correlation between EC and NO_2 was also found in autumn

Table 1
Statistics of $PM_{2.5}$ mass concentrations, its chemical constituents, b_{sp} and meteorological parameters.

	Annual (n = 123)	Spring (Apr-09) (n = 30)	Summer (Jul-09) (n = 31)	Autumn (Oct-09) (n = 31)	Winter (Jan-10) (n = 31)
$PM_{2.5}$/μg m^{-3}	76.8 ± 45.1	76.0 ± 25.3	38.6 ± 15.7	89.3 ± 34.7	103.3 ± 50.1
OC/μg m^{-3}	9.0 ± 5.1	8.3 ± 2.2	5.6 ± 2.3	10.4 ± 4.7	11.8 ± 7.3
EC/μg m^{-3}	6.0 ± 3.3	6.1 ± 2.3	3.5 ± 1.3	6.7 ± 2.7	7.8 ± 4.3
OC/EC	1.5 ± 0.4	1.5 ± 0.3	1.7 ± 0.5	1.5 ± 0.3	1.5 ± 0.3
Na^+/μg m^{-3}	2.2 ± 0.4	2.5 ± 0.3	2.1 ± 0.3	2.0 ± 0.3	2.1 ± 0.5
NH_4^+/μg m^{-3}	5.1 ± 3.3	6.0 ± 2.5	1.6 ± 1.2	6.4 ± 2.7	6.5 ± 3.4
K^+/μg m^{-3}	0.9 ± 0.5	1.0 ± 0.4	0.3 ± 0.1	1.1 ± 0.4	1.0 ± 0.5
Mg^{2+}/μg m^{-3}	LD[a]	LD	LD	LD	LD
Ca^{2+}/μg m^{-3}	0.4 ± 0.4	0.1 ± 0.3	0.2 ± 0.1	0.7 ± 0.2	0.6 ± 0.4
F^-/μg m^{-3}	LD	LD	LD	LD	LD
Cl^-/μg m^{-3}	1.8 ± 1.8	1.8 ± 1.3	1.0 ± 0.7	1.0 ± 0.7	3.3 ± 2.7
NO_3^-/μg m^{-3}	7.8 ± 7.2	9.9 ± 6.5	2.0 ± 1.0	6.4 ± 7.2	13.0 ± 7.1
SO_4^{2-}/μg m^{-3}	18.1 ± 9.5	17.8 ± 5.5	9.2 ± 4.6	27.5 ± 8.7	17.8 ± 8.0
b_{sp}/Mm^{-1}	326 ± 248	243 ± 93[b]	95 ± 46[c]	473 ± 222	469 ± 279
TEMP[d]/°C	24.7 ± 2.0	23.7 ± 0.6	26.0 ± 0.9	25.1 ± 0.6	22.5 ± 1.0
RH[d]/%	51 ± 11	51 ± 8	52 ± 3	55 ± 10	46 ± 15
WS/m s^{-1}	1.3 ± 0.9	1.5 ± 0.7	1.8 ± 0.7	0.3 ± 0.3	0.9 ± 0.5
TEMP[e]/°C	23.7 ± 6.1	22.6 ± 2.4	29.9 ± 1.6	27.1 ± 1.3	15.2 ± 4.0
RH[e]/%	64 ± 14	68 ± 12	68 ± 8	50 ± 12	71 ± 14
SR/W m^{-2}	153 ± 79	133 ± 68	215 ± 62	177 ± 45	77 ± 44
PR/mm	218.6	79.0	68.0	21.0	50.6
$PM_{2.5-10}$[f]	26.1 ± 28.6	56.8 ± 37.8	11.2 ± 13.1	18.4 ± 15.5	22.7 ± 21.7

[a] LD, low detection.
[b] Number was 25.
[c] Number was 30.
[d] Temperature and relative humidity in nephelometer.
[e] Temperature and relative humidity in ambient condition.
[f] $PM_{2.5-10} = PM_{10}-PM_{2.5}$.

($R^2 = 0.93$), and fairly good correlations were found in spring, summer and winter ($R^2 = 0.71$, 0.78 and 0.78, respectively) (figure not shown). These results suggest that vehicle emissions were the dominant sources of OC and EC. The highest OC/EC ratio (1.7) in summer may be related to the formation of secondary organic carbon (SOC) (Cao et al., 2004), which was another major component of OC. Relatively poor correlations between OC and NO_2 and between EC and NO_2 were found in spring, suggesting more complex sources of carbonaceous aerosols in spring than in other seasons. In short, carbon aerosols may be affected by vehicle emissions significantly. A ratio of organic mass to organic carbon (OM/OC) of 1.4 would be appropriate for an urban area with fresh emissions.

Water-soluble ions were also important fractions of $PM_{2.5}$. The sum of all the detected water-soluble ions was 36.2 ± 19.7 μg m^{-3}, accounting for 47.0 ± 7.2% of $PM_{2.5}$ mass. The average concentrations of the four anions followed the sequence of $SO_4^{2-} > NO_3^- > Cl^- > F^-$, while the five major cations followed the order of $NH_4^+ > Na^+ > K^+ > Ca^{2+} = Mg^{2+}$. SO_4^{2-}, NO_3^- and NH_4^+ dominated the water-soluble inorganic species, accounting for 83.3 ± 6.3% of the total ion concentration. Ion balance calculations are commonly used to evaluate the acid–base balance of aerosol particles. To calculate the cation/anion balance of $PM_{2.5}$, we converted the ion mass concentrations into microequivalents (Tao et al., 2013). As shown in Fig. 4, the anion/cation ratios, determined from the slopes of linear regressions for the seasonally stratified data, followed the order of autumn (1.68) > summer (1.43) > winter (1.38) > spring (1.33). Most samples had an anion/cation (A/C) ratio evidently higher than 1.00, which indicated weakly acidic particles.

To further evaluate the impact of various chemical components of $PM_{2.5}$ on b_{sp}, the $PM_{2.5}$ mass was reconstructed based on OM, EC, inorganic ions, water, and FS. Water concentrations were estimated by the online version of the E-AIM model (Model III) (http://www.aim.env.uea.ac.uk/aim/model3/model3a.php) at a fixed relative humidity (40%) and temperature (25 °C). The reconstructed $PM_{2.5}$ concentrations were presented in Fig. 5. The Pearson correlation coefficients between measured and reconstructed $PM_{2.5}$ mass concentrations were larger than 0.95 and the slopes ranged from 0.96 to 1.12 during the four seasons, indicating that OM, EC, FS, water, and inorganic ions were dominant species and the total mass of these species could closely represent the measured $PM_{2.5}$. On average, the reconstructed mass accounted for 93.2% of the measured $PM_{2.5}$ mass in the urban area of Guangzhou, although larger by 3.0% during autumn. OM, EC, inorganic ions, water, and FS accounted for 17.2%, 8.1%, 47.0%, 11.1% and 9.8%, respectively, of the total $PM_{2.5}$ mass. Considering that the filters were weighted at RH between 35% and 45%, water contents were calculated at RH 40%. Therefore, the uncertainty of water content in $PM_{2.5}$ should be the largest among all the sources for reconstructing $PM_{2.5}$ (Malm et al., 2011). Overall, the determined chemical compositions in $PM_{2.5}$ can represent the total $PM_{2.5}$ mass.

3.2. Aerosol light scattering and its relationship with $PM_{2.5}$

Annual average b_{sp} was 326 ± 248 Mm^{-1}, with daily values ranging from 55 to 1354 Mm^{-1}. Seasonal variations of b_{sp} ranked in the order of autumn (473 Mm^{-1}) > winter (469 Mm^{-1}) > spring (243 Mm^{-1}) > summer (95 Mm^{-1}) (Table 1). b_{sp} in autumn slightly increased compared with

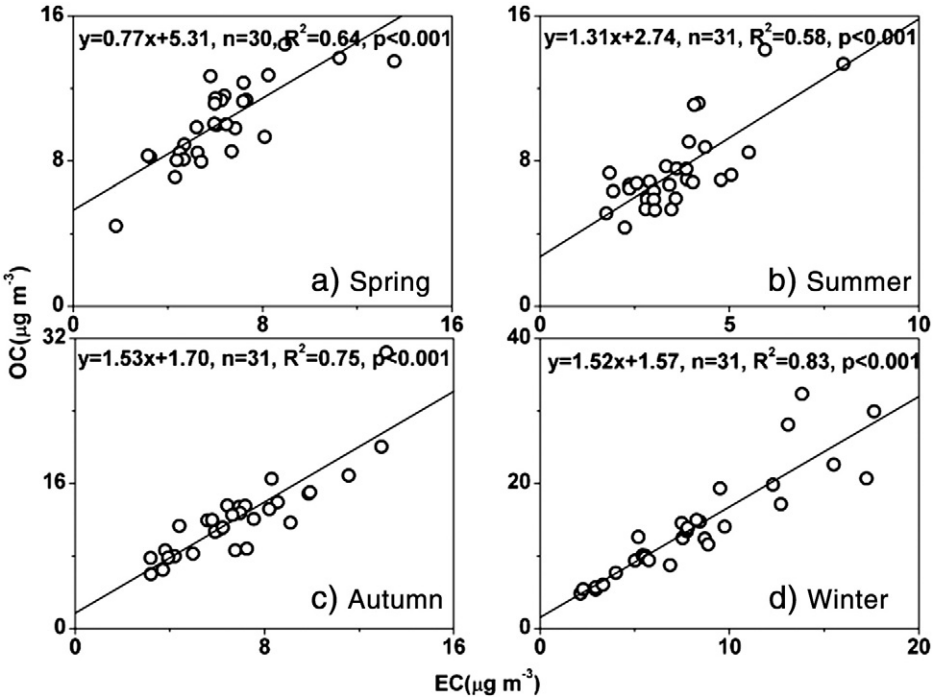

Fig. 3. Correlations between OC and EC in the four seasons.

that measured in the same season of 2004 at a Guangzhou urban site (Andreae et al., 2008), which revealed that visibility degradation has not been improved in the past five years in this city. b_{sp} observed in Guangzhou was within the range of several existing studies in Asia, e.g., much higher than those at a Shanghai urban site in winter (293 Mm^{-1}) (Xu et al., 2012) and at a Lin'an rural site in autumn (353 Mm^{-1}) (Xu et al., 2002), evidently lower than those at a Xi'an urban site in all the four seasons (434 Mm^{-1}, 454 Mm^{-1}, 606 Mm^{-1}, and 657 Mm^{-1}, respectively, in spring, summer, autumn and

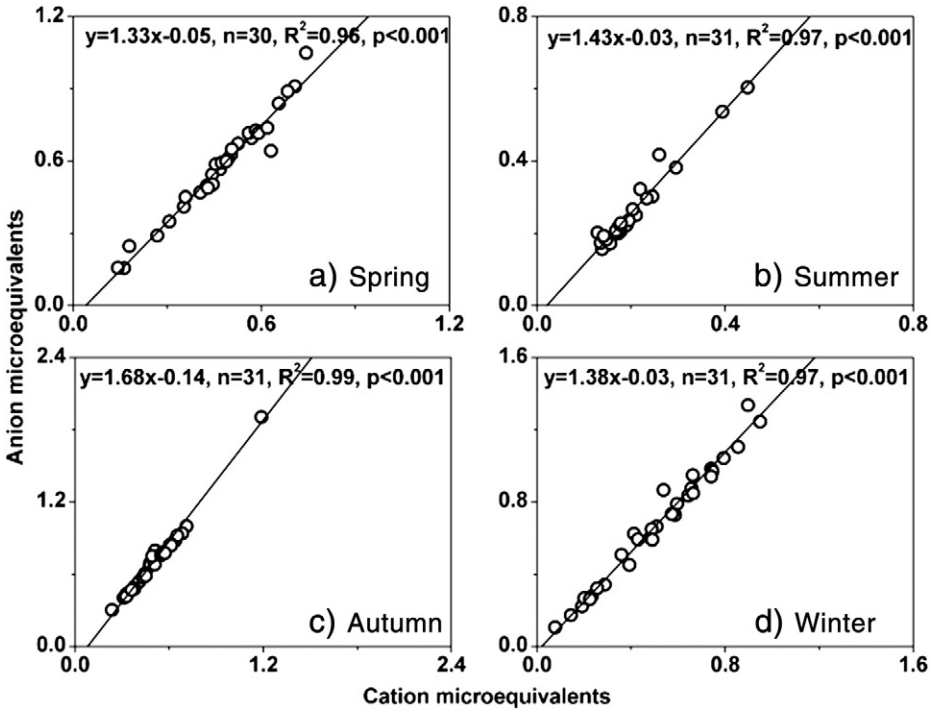

Fig. 4. Scatter plot of major anions versus major cations.

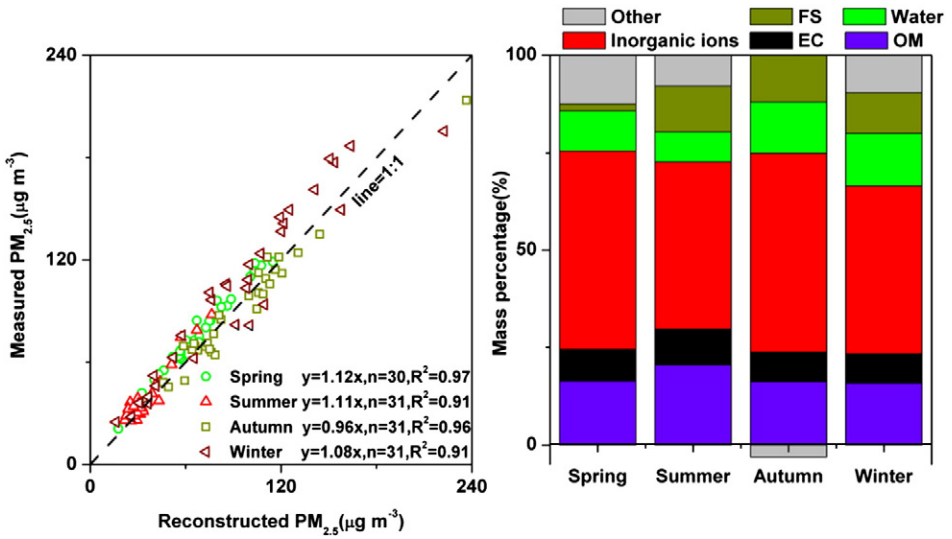

Fig. 5. Reconstructed $PM_{2.5}$ mass concentrations in four seasons.

winter) (Cao et al., 2012), lower than that at a rural site in Shangdianzi, Beijing in summer (190 Mm^{-1}) (Yan et al., 2008), and also lower than those at several coast sites (242 Mm^{-1} and 227 Mm^{-1}, respectively, in Junnong and Yonghyun) in Korea in summer (Kim et al., 2006).

Aerosol MSE is an important parameter in global circulation and chemical transport models for computing radiative forcing of aerosols and chemical extinction budgets used for visibility regulatory purposes (Hand and Malm, 2007). Regression of the measured b_{sp} against $PM_{2.5}$ mass concentration yields an average MSE that can be simplified as $b_{sp}/PM_{2.5}$ ($m^2\ g^{-1}$). In fact, $b_{sp}/PM_{2.5}$ is not the real $PM_{2.5}$ MSE since b_{sp} was not measured with a $PM_{2.5}$ inlet. Considering that the contribution of CM to b_{sp} is very small (see Section 3.3), $b_{sp}/PM_{2.5}$ can be a good approximation of $PM_{2.5}$ MSE. $PM_{2.5}$ MSE can be a measure of particle scattering properties and be used to estimate b_{sp} when $PM_{2.5}$ mass is known. In this study, $PM_{2.5}$ mass concentrations were obtained under a dry condition (RH = 40%); however, b_{sp} were measured at RH < 70% during the four seasons. b_{sp} may be enhanced by hygroscopic growth as a function of RH unless it was measured under dry conditions. In this study, most b_{sp} samples were measured at RH > 40%, especially in summer. Thus, to minimize the impact of particle hygroscopic growth on b_{sp}, we selected b_{sp} data that were measured at RH < 50% to investigate the seasonal variations of $PM_{2.5}$ MSE. The average $PM_{2.5}$ MSE was determined to be 3.5 ± 0.9 $m^2\ g^{-1}$ at RH < 50%. Apparent seasonal variations were found, following the sequence of autumn (4.5 ± 0.2 $m^2\ g^{-1}$) > winter (3.9 ± 0.5 $m^2\ g^{-1}$) > spring (3.0 ± 0.4 $m^2\ g^{-1}$) > summer (2.3 ± 0.3 $m^2\ g^{-1}$). Although only data at RH < 50% was used for calculating the $PM_{2.5}$ MSE, the derived values were close to those found in previous studies conducted in Guangzhou, e.g., in autumn (4.2 ± 1.0 $m^2\ g^{-1}$) (Andreae et al., 2008) and in summer (2.7 ± 0.7 $m^2\ g^{-1}$) (Jung et al., 2009a). In general, the higher $PM_{2.5}$ MSE in autumn and winter periods should be due to the increased b_{sp} or $PM_{2.5}$, as can be explained by the growth of particles into size ranges with higher scattering efficiencies under more polluted conditions (Lowenthal and Kumar, 2004; Jung et al., 2009a,b).

3.3. Source apportionment of b_{sp}

To determine the relationship between b_{sp} and the chemical components of $PM_{2.5}$, b_{sp} was reconstructed in each season according to the original IMPROVE formula with a modification described in Section 2.5 (for simplicity, it is still referred to as the original IMPROVE formula below). RH data from nephelometer inner relative humidity detector was introduced in the calculation of $f_L(RH)$ and $f_{SS}(RH)$. The estimated b_{sp} using the original IMPROVE formula and the measured b_{sp} correlated well ($R^2 > 0.84$) during all the four seasons (Fig. 6). The slopes of the regression between the estimated and the measured b_{sp} were close to 1.00 in spring (0.88) and summer (1.06), but deviated from 1 significantly in autumn (0.53) and winter (0.53). On annual average, b_{sp} was underestimated by 22 ± 28% using the original formula. These results suggested that the chemical component MSEs may not be constant from season to season.

To further investigate the chemical component MSEs in different seasons, multiple linear regression of measured b_{sp} against the $(NH_4)_2SO_4$, NH_4NO_3, OM, SS, FS, and CM were performed in the four seasons. The amount of scattering associated with individual species can be estimated statistically using:

$$b_{sp}(RH) = a_1 f_L(RH)[(NH_4)_2SO_4] + a_3 f_L(RH)[NH_4NO_3] + a_4[OM] + a_2 f_{SS}(RH)[SS] + a_5[FS] + a_6[CM] \quad (3)$$

where the calculation methods of $(NH_4)_2SO_4$, NH_4NO_3, OM, SS, FS, and CM concentrations are the same as in Eq. (2).

It was found that, if applying annual average data in the above equation, using the calculated MSEs of individual chemical components cannot reconstruct the measured b_{sp} well with the slopes deviated from 1.00 significantly, although the correlations between the estimated and the measured b_{sp} were very well (figure not presented). Considering that the $PM_{2.5}$ MSEs showed evident seasonal variations (see Section 3.2 above), the MSEs of each chemical species were then estimated using seasonal data. The MSEs were estimated by the stepwise

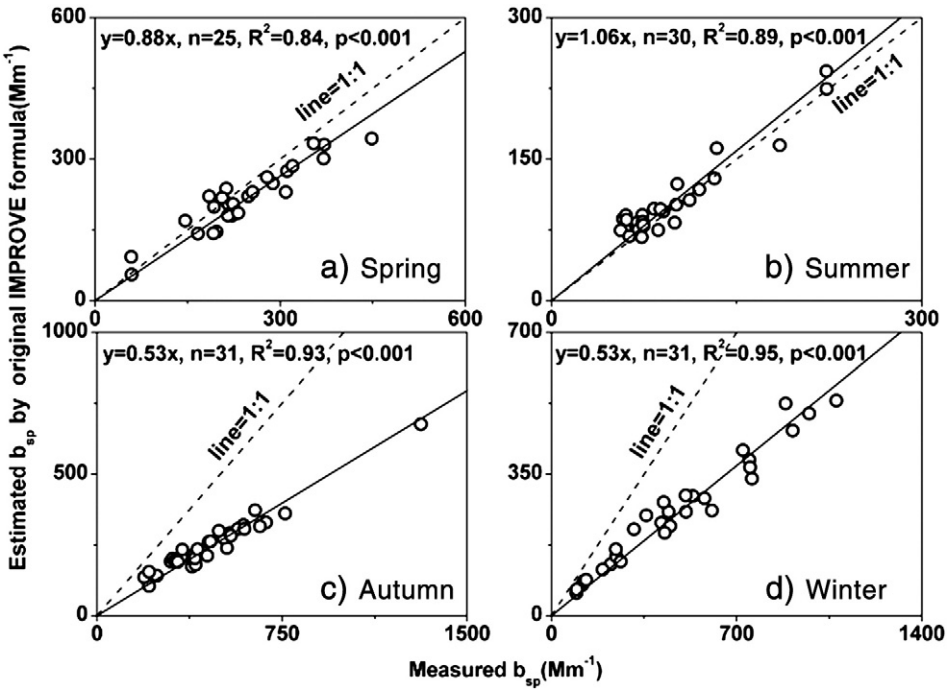

Fig. 6. Estimated b_{sp} by the original IMPROVE formula versus measured b_{sp} in four seasons.

multiple linear regression through self-compiled MATLAB program. The constraints of the multiple linear regression results were as follows: the calculated MSEs and R^2 must be larger than zero and 0.90, respectively; the slopes between the estimated and the measured b_{sp} must be in the range of 0.95 and 1.05. The calculation step is 0.1.

The estimated seasonal average MSEs of $(NH_4)_2SO_4$, NH_4NO_3, OM, SS, FS and CM are summarized in Table 2 and the sum of the estimated individual b_{sp} is compared with measured ones in Fig. 7. The estimated and the measured b_{sp} correlated very well with R^2 larger than 0.9 in all the seasons. The slopes of the regressions were all close to 1.0. The estimated MSEs of $(NH_4)_2SO_4$, NH_4NO_3, and OM were much higher in autumn and winter than in spring and summer, which can be explained by their seasonal mass concentrations (Malm et al., 2003). The seasonal variations of $(NH_4)_2SO_4$, NH_4NO_3, and OM MSEs were mostly similar to those of $PM_{2.5}$; the only exception was autumn–winter comparison which showed an opposite trend (compare Table 2 with those described in Section 3.2). This was mainly caused by the exclusion of some chemical components, which had much higher concentrations in winter than in autumn based on $PM_{2.5}$ mass reconstruction, in the b_{sp} regression calculation. Besides, the measured b_{sp} did not differ significantly between winter and autumn (1% difference as shown in Table 1). Thus, $(NH_4)_2SO_4$, NH_4NO_3, and OM MSEs in winter were systematically increased by the regression model.

The SS MSE in summer was 1.5 $m^2\ g^{-1}$, lower than in any other season (2.1 to 2.6), but was close to the value of 1.8 $m^2\ g^{-1}$ in IMPROVE formula. This suggests that Cl^- in summer was mainly from sea salt aerosols and distributed mainly in the coarse particle (>2.5 μm) while in other seasons Cl^- from other sources such as coal combustion and biomass burning was also significant and distributed in fine particle (<2.5 μm) in other seasons (Yao et al., 2003; Zhang et al., 2008; Yao and Zhang, 2012; Tao et al., 2013). This conclusion was supported by the mass size-distribution data we collected at SCIES site (data to be published in a separate study).

On annual average, the estimated b_{sp} from using the regression equation was overestimated by 4 ± 12% compared to measurements. $(NH_4)_2SO_4$, NH_4NO_3, OM, SS, FS and CM accounted for 50 ± 11%, 18 ± 10%, 19 ± 5%, 5 ± 4%, 3 ± 2% and 5 ± 6%, respectively, of the estimated b_{sp}. The percentage contributions to the estimated b_{sp} varied significantly with season from species of $(NH_4)_2SO_4$, NH_4NO_3 and OM, although this was not the case from SS, FS and CM (Fig. 7). Looking at the seasonal variations of the percentage contributions to the estimated b_{sp} from the individual species, it was found that the evidently higher value was 64% in autumn from $(NH_4)_2SO_4$, 27% in winter from NH_4NO_3, 8% in summer from SS, and 23% in summer from OM. Factors discussed in Section 3.1 explain the above seasonal patterns. For example, the highest seasonal power plant emissions in autumn in PRD caused high seasonal

Table 2
Estimated mass scattering efficiencies of individual species by stepwise multiple linear regression.

	Spring (Apr-09) (n = 25)	Summer (Jul-09) (n = 30)	Autumn (Oct-09) (n = 31)	Winter (Jan-10) (n = 31)
$(NH_4)_2SO_4/m^2\ g^{-1}$	2.9 ± 0.8	2.5 ± 0.8	4.8 ± 0.5	5.3 ± 0.7
$NH_4NO_3/m^2\ g^{-1}$	3.2 ± 0.3	2.6 ± 0.6	4.9 ± 0.7	5.5 ± 0.7
$OM/m^2\ g^{-1}$	3.3 ± 0.9	2.8 ± 0.5	5.1 ± 0.9	6.2 ± 0.5
$SS/m^2\ g^{-1}$	2.1 ± 0.4	1.5 ± 0.4	2.6 ± 0.6	2.4 ± 0.9
$FS/m^2\ g^{-1}$	1.1 ± 0.6	0.9 ± 0.4	1.3 ± 0.6	0.7 ± 0.5
$CM/m^2\ g^{-1}$	0.5 ± 0.2	0.6 ± 0.3	0.6 ± 0.5	0.5 ± 0.4

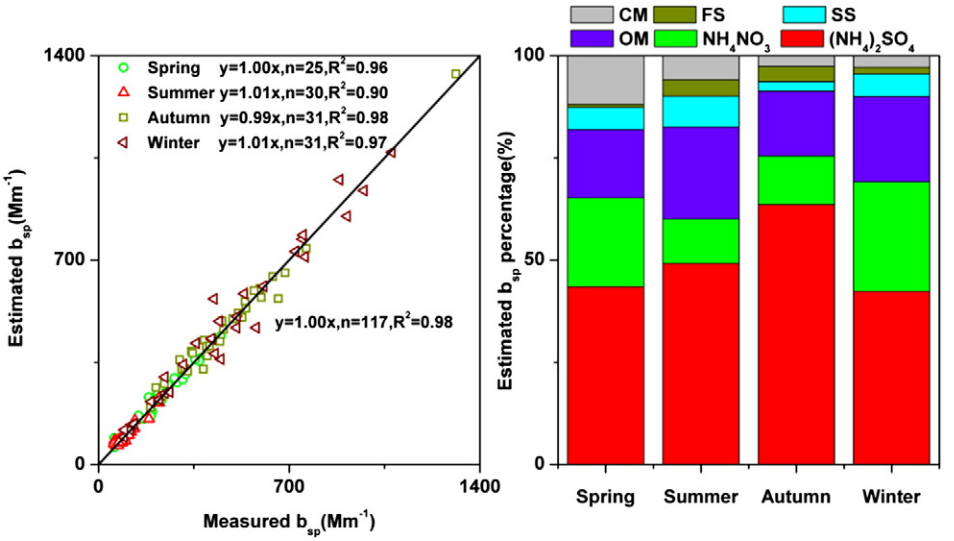

Fig. 7. Correlations between the estimated and measured b_{sp}, and their load percentages in four seasons.

$(NH_4)_2SO_4$ concentrations; low temperature in winter favored NH_4NO_3 formation; air masses from China South Sea in summer brought in sea salt; and high temperature in summer favored SOC formation.

Potential uncertainties in the results presented above can come from data collection process (instruments), laboratory chemical analysis, and theoretically explanation of the data. The total uncertainty (U_{total}) can be estimated from known uncertainties of individual sources (U_i) using Eq. (4), which was recommended by IPCC (Intergovernmental Panel on Climate Change).

$$U_{total} = \left(\Sigma U_i^2\right)^{1/2}. \quad (4)$$

The U_{total} of the estimated b_{sp} obtained from Eq. (3) were found to be 81%, 84%,101%, and 115%, respectively, in spring, summer, autumn and winter.

4. Conclusions

$PM_{2.5}$, its major chemical components (OC, EC and water-soluble ions), and b_{sp} were measured from April 2009 to January 2010 at an urban site in Guangzhou. The annual average $PM_{2.5}$ mass concentration was 76.8 ± 41.5 μg m^{-3}, with OM, EC, inorganic salts, water, and FS contributed 20.8%, 8.1%, 46.8%, 13.0% and 9.7%, respectively. Annual average $PM_{2.5}$ MSE was 3.5 ± 0.9 m^2 g^{-1}, with obvious seasonal variations following the order of autumn (4.5 ± 0.2 m^2 g^{-1}) > winter (3.9 ± 0.5 m^2 g^{-1}) > spring (3.0 ± 0.4 m^2 g^{-1}) > summer (2.3 ± 0.3 m^2 g^{-1}). High $PM_{2.5}$ MSE in autumn and winter should be due to high levels of b_{sp} and $PM_{2.5}$.

The slopes of the regression between the estimated b_{sp} from using the original IMPROVE formula (with a modification of including sea salt aerosols) and the measured b_{sp} were close to 1 in spring and summer, but deviated significantly from 1 in autumn and winter. On annual average, b_{sp} derived from the original formula was 22 ± 28% lower than the measured value. These results suggest that the chemical component MSEs may not be constant from season to season.

A multiple linear regression equations of the measured b_{sp} against $(NH_4)_2SO_4$, NH_4NO_3, OM, SS, FS, and CM were derived in four seasons. The estimated b_{sp} by the multiple linear regression equations were close to the measured b_{sp} in four seasons. Based on the regression model results, $(NH_4)_2SO_4$, NH_4NO_3, OM, SS, FS and CM accounted for 50 ± 11%, 18 ± 10%, 19 ± 5%, 5 ± 4%, 3 ± 2% and 5 ± 6%, respectively, of the estimated b_{sp}. It is noticed that the uncertainties in this estimation could be larger than the differences between the estimated and the measured values. Therefore, the method should only be considered as a first-order estimation.

Acknowledgments

We appreciate the valuable comments from anonymous reviewers which helped us improve the manuscript. This study was supported by the Special Scientific Research Funds for Environment Protection Commonweal Section (No. 201409009), the Ministry of Science, Technology of China (2010DFA22770), and the National Basic Research Program of China (2010CB428503 and 2013FY112700). The authors would like to express their sincere appreciation for their financial support to accomplish this study.

References

Aldabe, J., Elustondo, D., Santamaría, C., Lasheras, E., Pandolfi, M., Alastuey, A., Querol, X., Santamaría, J.M., 2011. Chemical characterisation and source apportionment of $PM_{2.5}$ and PM_{10} at rural, urban and traffic sites in Navarra (North of Spain). Atmos. Res. 102, 191–205.

Amato, F., Hopke, P.K., 2012. Source apportionment of the ambient $PM_{2.5}$ across St. Louis using constrained positive matrix factorization. Atmos. Environ. 46, 329–337.

Anderson, T.L., Ogren, J.A., 1998. Determining aerosol radiative properties using the TSI 3563 integrating nephelometer. Aerosol Sci. Technol. 29, 57–69.

Andreae, M.O., Schmid, O., Yang, H., Chan, D.L., Yu, J.Z., Zeng, L.M., Zhang, Y.H., 2008. Optical properties and chemical composition of the atmospheric aerosol in urban Guangzhou, China. Atmos. Environ. 42, 6335–6350.

Cao, J.J., Lee, S.C., Ho, K.F., Zhang, X.Y., Zou, S.C., Fung, K., Chow, J.C., Watson, J.G., 2003. Characteristics of carbonaceous aerosol in Pearl River Delta Region, China during 2001 winter period. Atmos. Environ. 37, 1451–1460.

Cao, J.J., Lee, S.C., Ho, K.F., Zou, S.C., Fung, K.K., Li, Y., Watson, J.G., Chow, J.C., 2004. Spatial and seasonal variations of atmospheric organic carbon and elemental carbon in Pearl River Delta Region, China. Atmos. Environ. 38, 4447–4456.

Cao, J.J., Lee, S.C., Chow, J.C., Watson, J.G., Ho, K.F., Zhang, R.J., Jin, Z.D., Shen, Z.X., Chen, G.C., Kang, Y.M., Zou, S.C., Zhang, L.Z., Qi, S.H., Dai, M.H., Cheng, Y., Hu, K., 2007. Spatial and seasonal distributions of carbonaceous aerosols over China. J. Geophys. Res. 112 (D22). http://dx.doi.org/10.1029/2006JD008205.

Cao, J.J., Wang, Q.Y., Chow, J.C., Watson, J.G., Tie, X.X., Shen, Z.X., Wang, P., An, Z.S., 2012. Impacts of aerosol compositions on visibility impairment in Xi'an, China. Atmos. Environ. 59, 559–566.

Cheng, Y.F., Wiedensohler, A., Eichler, H., Su, H., Gnauk, T., Brüggemann, E., Herrmann, H., Heintzenberg, J., Slanina, J., Tuch, T., Hu, M., Zhang, Y.H., 2008. Aerosol optical properties and related chemical apportionment at Xinken in Pearl River Delta of China. Atmos. Environ. 42, 6351–6372.

Cheung, H.C., Wang, T., Baumann, K., Guo, H., 2005. Influence of regional pollution outflow on the concentrations of fine particulate matter and visibility in the coastal area of southern china. Atmos. Environ. 39, 6463–6474.

Chow, J.C., Watson, J.G., Lowenthal, D.H., Magliano, K.L., 2005. Loss of $PM_{2.5}$ nitrate from filter samples in central California. J. Air Waste Manag. Assoc. 55 (8), 1158–1168.

Chow, J.C., Watson, J.G., Chen, L.W., Chang, M.C., Robinson, N.F., Trimble, D., Kohl, S., 2007. The IMPROVE_A temperature protocol for thermal/optical carbon analysis: maintaining consistency with a long-term database. J. Air Waste Manag. Assoc. 57, 1014–1023.

Deng, X.J., Tie, X.X., Wu, D., Zhou, X.J., Bi, X.Y., Tan, H.B., Li, F., Hang, C.L., 2008. Long-term trend of visibility and its characterizations in the Pearl River Delta (PRD) region, China. Atmos. Environ. 42, 1424–1435.

Dockery, D.W., Pope, C.A., 1994. Acute respiratory effects of particulate air pollution. Annu. Rev. Public Health 15, 107–132.

Duan, F.K., He, K.B., Ma, Y.L., Yang, F.M., Yu, X.C., Cadle, S.H., Chan, T., Mulawa, P.A., 2006. Concentration and chemical characteristics of $PM_{2.5}$ in Beijing, China: 2001–2002. Sci. Total. Environ. 355, 264–275.

Feng, Y.L., Chen, Y.J., Guo, H., Zhi, G.R., Xiong, S.C., Li, J., Sheng, G.Y., Fu, J.M., 2009. Characteristics of organic and elemental carbon in $PM_{2.5}$ samples in Shanghai, China. Atmos. Res. 92, 434–442.

Hand, J.L., Malm, W.C., 2007. Review of aerosol mass scattering efficiencies from ground-based measurements since 1990. J. Geophys. Res. 112, D16203. http://dx.doi.org/10.1029/2007JD008484.

Jung, J., Lee, H., Kim, Y.J., Liu, X., Zhang, Y., Gu, J., Fan, S., 2009a. Aerosol chemistry and the effect of aerosol water content on visibility impairment and radiative forcing in Guangzhou during the 2006 Pearl River Delta campaign. J. Environ. Manag. 90, 3231–3244.

Jung, J., Lee, H., Kim, Y.J., Liu, X., Zhang, Y., Hu, M., Sugimoto, N., 2009b. Optical properties of atmospheric aerosols obtained by in situ and remote measurements during 2006 Campaign of Air Quality Research in Beijing (CAREBeijing-2006). J. Geophys. Res. 114 (D00G02). http://dx.doi.org/10.1029/2008JD010337.

Kim, Y.J., Kim, K.W., Kim, S.D., Lee, B.K., Han, J.S., 2006. Fine particulate matter characteristics and its impact on visibility impairment at two urban sites in Korea: Seoul and Incheon. Atmos. Environ. 40, S593–S605.

Laden, F., Neas, L.M., Dockery, D.W., Schwartz, J., 2000. Association of fine Ppticulate matter from different sources with daily mortality in six U.S. Cities. Environ. Heal. Perspect. 108 (10), 941–947.

Lin, Z.J., Tao, J., Chai, F.H., Fan, S.J., Yue, J.H., Zhu, L.H., Ho, K.F., Zhang, R.J., 2013. Impact of relative humidity and particles number size distribution on aerosol light extinction in the urban area of Guangzhou. Atmos. Chem. Phys. 13, 1115–1128.

Lowenthal, D.H., Kumar, N., 2003. $PM_{2.5}$ Mass and Light Extinction Reconstruction in IMPROVE. J. Air Waste Manag. Assoc. 53, 1109–1120.

Lowenthal, D.H., Kumar, N., 2004. Variation of mass scattering efficiencies in IMPROVE. J. Air Waste Manag. Assoc. 54, 926–934.

Malm, W.C., Sisler, J.F., Huffman, D., Eldred, R.A., Cahill, T.A., 1994. Spatial and seasonal trends in particle concentration and optical extinction in the United States. J. Geophys. Res. 99 (D1), 1347–1370.

Malm, W.C., Day, D.E., Kreidenweis, S.M., Collett, J.L., Lee, T., 2003. Humidity-dependent optical properties of fine particles during the Big Bend Regional Aerosol and Visibility Observational study. J. Geophys. Res. 108 (D9), 4279. http://dx.doi.org/10.1029/2002JD002998.

Malm, W.C., Schichtel, B.A., Pitchford, M.L., 2011. Uncertainties in $PM_{2.5}$ gravimetric and speciation measurements and what we can learn from them. J. Air Waste Manag. Assoc. 61, 1131–1149.

Pitchford, M., Malm, W., Schichtel, B., Kumar, N., Lowenthal, D., Hand, J., 2007. Revised algorithm for estimating light extinction from improve particle speciation data. J. Air Waste Manag. Assoc. 57, 1326–1336.

Pope, C.A., Dockery, D.W., 2006. Health effects of fine particulate air pollution: lines that connect. J. Air Waste Manag. Assoc. 56, 709–742.

Samet, J.M., Dominici, F., Curriero, F.C., Coursac, I., Zeger, S.L., 2000. Fine particulate air pollution and mortality in U.S. cities, 1987–1994. N. Engl. J. Med. 343 (24), 1742–1749.

Shen, Z.X., Cao, J.J., Arimoto, R., Han, Z.W., Zhang, R.J., Han, Y.M., Liu, S.X., Okuda, T., Nakao, S., Tanaka, S., 2009. Ionic composition of TSP and $PM_{2.5}$ during dust storms and air pollution episodes at Xi'an, China. Atmos. Environ. 43, 2911–2918.

Tan, J.H., Duan, J.C., Chen, D.H., Wang, X.H., Guo, S.J., Bi, X.H., Sheng, G.Y., He, K.B., Fu, J.M., 2009. Chemical characteristics of haze during summer and winter in Guangzhou. Atmos. Res. 94, 238–245.

Tao, J., Ho, K.F., Chen, L.G., Zhu, L.H., Han, J.L., Xu, Z.C., 2009. Effect of chemical composition of $PM_{2.5}$ on visibility in Guangzhou, China, 2007 spring. Particuology 7, 68–75.

Tao, J., Shen, Z.X., Zhu, C.S., Yue, J.H., Cao, J.J., Liu, S.X., Zhu, L.H., Zhang, R.J., 2012. Seasonal variations and chemical characteristics of sub-micrometer particles (PM_1) in Guangzhou, China. Atmos. Res. 118, 222–231.

Tao, J., Zhang, L.M., Engling, G., Zhang, R.J., Yang, Y.H., Cao, J.J., Zhu, C.S., Wang, Q.Y., Luo, L., 2013. Chemical Composition of $PM_{2.5}$ in an urban environment in Chengdu, China: Importance of springtime dust storms and biomass burning. Atmos. Res. 122, 270–283.

Turpin, B.J., Huntzicker, J.J., 1995. Identification of secondary aerosol episodes and quantification of primary and secondary organic aerosol concentrations during SCAQS. Atmos. Environ. 29, 3527–3544.

Wang, X., Zhang, L., Moran, M.D., 2010. Uncertainty assessment of current size-resolved parameterizations for below-cloud particle scavenging by rain. Atmos. Chem. Phys. 10, 5685–5705.

Watson, J.G., 2002. Visibility: science and regulation. J. Air Waste Manag. Assoc. 52, 628–713.

Watson, J.G., Chow, J.C., Houck, J.E., 2001. $PM_{2.5}$ chemical source profiles for vehicle exhaust, vegetative burning, geological material, and coal burning in northwestern Colorado during 1995. Chemosphere 43, 1141–1151.

Watson, J.G., Chow, J.C., Lowenthal, D.H., Magliano, K.L., 2008. Estimating aerosol light scattering at the Fresno Supersite. Atmos. Environ. 42, 1186–1196.

Xu, J., Bergin, M.H., Yu, X., Liu, G., Zhao, J., Carrico, C.M., Baumann, K., 2002. Measurement of aerosol chemical, physical, and radiative properties in the Yangtze delta region of China. Atmos. Environ. 2002 (36), 161–173.

Xu, J., Tao, J., Zhang, R., Cheng, T., Leng, C., Chen, J., Huang, G., Li, X., Zhu, Z., 2012. Measurements of surface aerosol optical properties in winter of Shanghai. Atmos. Res. 109–110, 25–35.

Yan, P., Tang, J., Huang, J., Mao, J.T., Zhou, X.J., Liu, Q., Wang, Z.F., Zhou, H.G., 2008. The measurement of aerosol optical properties at a rural site in Northern China. Atmos. Chem. Phys. 8, 2229–2242.

Yang, L., Wang, D., Cheng, S., Wang, Z., Zhou, Y., Zhou, X., Wang, W., 2007. Influence of meteorological conditions and particulate matter on visual range impairment in Jinan, China. Sci. Total. Environ. 383, 164–173.

Yao, X., Zhang, L., 2012. Chemical processes in sea-salt chloride depletion observed at a Canadian rural coastal site. Atmos. Environ. 46, 189–194.

Yao, X.H., Lau, A.P.S., Fang, M., Chan, C.K., Hu, M., 2003. Size distributions and formation of ionic species in atmospheric particulate pollutants in Beijing, China: 1 — inorganic ions. Atmos. Environ. 37, 2991–3000.

Yao, T.T., Huang, X.F., He, L.Y., Hu, M., Sun, T.L., Xue, L., Lin, Y., Zeng, L.W., Zhang, Y.H., 2010. High time resolution observation and statistical analysis of atmospheric light extinction properties and the chemical speciation of fine particulates. Sci. China 53 (8), 1801–1808.

Yu, H., Wu, C., Wu, D., Yu, J.Z., 2010. Size distributions of elemental carbon and its contribution to light extinction in urban and rural locations in the Pearl River Delta Region, China. Atmos. Chem. Phys. 10, 5107–5119.

Zhang, R.J., Cao, J.J., Lee, S.C., Shen, Z.X., Ho, K.F., 2007. Carbonaceous aerosols in PM_{10} and pollution gases in winter in Beijing. J. Environ. Sci. 19, 564–571.

Zhang, L., Vet, R., Wiebe, A., Mihele, C., Sukloff, B., Chan, E., Moran, M.D., Iqbal, S., 2008. Characterization of the size-segregated water-soluble inorganic ions at eight Canadian rural sites. Atmos. Chem. Phys. 8, 7133–7151.

Zhang, T., Cao, J.J., Tie, X.X., Shen, Z.X., Liu, S.X., Ding, H., Han, Y.M., Wang, G.H., Ho, K.F., Qiang, J., Li, W.T., 2011. Water-soluble ions in atmospheric aerosols measured in Xi'an, China: seasonal variations and sources. Atmos. Res. 102, 110–119.

Zhang, F., Xu, L., Chen, J., Yu, Y., Niu, Z., Yin, L., 2012. Chemical compositions and extinction coefficients of $PM_{2.5}$ in peri-urban of Xiamen, China, during June 2009–May 2010. Atmos. Res. 106, 150–158.

Zheng, J., Zhang, L., Che, W., Zheng, Z., Yin, S., 2009. A highly resolved temporal and spatial air pollutant emission inventory for the Pearl River Delta region, China and its uncertainty assessment. Atmos. Environ. 43, 5112–5122.